

Gradient flow scale-setting with $N_f = 2 + 1 + 1$ Wilson-clover twisted-mass fermions

**C. Alexandrou,^{a,b} S. Bacchio,^b G. Bergner,^c P. Dimopoulos,^d J. Finkenrath,^b
R. Frezzotti,^e M. Garofalo,^{f,g} B. Kostrzewa,^{h,*} G. Koutsou,^b P. Labus,ⁱ F. Sanfilippo,^j
S. Simula,^j M. Ueding,^f C. Urbach^f and U. Wenger^k**

^a*Department of Physics, University of Cyprus, 20537 Nicosia, Cyprus*

^b*Computation-based Science and Technology Research Center, The Cyprus Institute, 20 Konstantinou Kavafi Street, 2121 Nicosia, Cyprus*

^c*University of Jena, Institute for Theoretical Physics, Max-Wien-Platz 1, D-07743 Jena, Germany*

^d*Dipartimento di Scienze Matematiche, Fisiche e Informatiche, Università di Parma and INFN, Gruppo Collegato di Parma, Parco Area delle Scienze 7/a (Campus), I-43124 Parma, Italy*

^e*Dipartimento di Fisica, Università di Roma "Tor Vergata" and INFN, Sezione di Tor Vergata, Via della Ricerca Scientifica 1, I-00133 Roma, Italy*

^f*HISKP (Theory), Rheinische Friedrich-Wilhelms-Universität Bonn, Nussallee 14-16, D-53115 Bonn, Germany*

^g*Dipartimento di Fisica, Università Roma Tre and INFN, Sezione di Roma Tre, Via della Vasca Navale 84, I-00146 Rome, Italy*

^h*High Performance Computing and Analytics Lab, Rheinische Friedrich-Wilhelms-Universität Bonn, Friedrich-Hirzebruch-Allee 8, D-53115 Bonn, Germany*

ⁱ*Fraunhofer Institute for Industrial Mathematics (ITWM), Fraunhofer-Platz 1, D-67663 Kaiserslautern, Germany*

^j*Istituto Nazionale di Fisica Nucleare, Sezione di Roma Tre, Via della Vasca Navale 84, I-00146 Rome, Italy*

^k*Institute for Theoretical Physics, Albert Einstein Center for Fundamental Physics, University of Bern, Sidlerstrasse 5, CH-3012 Bern, Switzerland*

E-mail: kostrzewab@informatik.uni-bonn.de

We present a determination of the gradient flow scales w_0 , $\sqrt{t_0}$ and t_0/w_0 in isosymmetric QCD, making use of the gauge ensembles produced by the Extended Twisted Mass Collaboration (ETMC) with $N_f = 2 + 1 + 1$ flavours of Wilson-clover twisted-mass quarks including configurations close to the physical point for all dynamical flavours. The simulations are carried out at three values of the lattice spacing and the scale is set through the PDG value of the pion decay constant, yielding $w_0 = 0.17383(63)$ fm, $\sqrt{t_0} = 0.14436(61)$ fm and $t_0/w_0 = 0.11969(62)$ fm. Finally, fixing the kaon mass to its isosymmetric value, we determine the ratio of the kaon and pion leptonic decay constants to be $f_K/f_\pi = 1.1995(44)$.

*The 38th International Symposium on Lattice Field Theory, LATTICE2021 26th-30th July, 2021
Zoom/Gather@Massachusetts Institute of Technology*

*Speaker

ensemble	β	V/a^4	a (fm)	$a\mu_\ell$	M_π (MeV)	L (fm)	$M_\pi L$
cA211.53.24	1.726	$24^3 \times 48$	0.0947 (4)	0.00530	346.4 (1.6)	2.27	3.99
cA211.40.24		$24^3 \times 48$		0.00400	301.6 (2.1)	2.27	3.47
cA211.30.32		$32^3 \times 64$		0.00300	261.1 (1.1)	3.03	4.01
cA211.12.48		$48^3 \times 96$		0.00120	167.1 (0.8)	4.55	3.85
cB211.25.24	1.778	$24^3 \times 48$	0.0816 (3)	0.00250	259.2 (3.0)	1.96	2.57
cB211.25.32		$32^3 \times 64$		0.00250	253.3 (1.4)	2.61	3.35
cB211.25.48		$48^3 \times 96$		0.00250	253.0 (1.0)	3.92	5.02
cB211.14.64		$64^3 \times 128$		0.00140	189.8 (0.7)	5.22	5.02
cB211.072.64		$64^3 \times 128$		0.00072	136.8 (0.6)	5.22	3.62
cC211.06.80	1.836	$80^3 \times 160$	0.0694 (3)	0.00060	134.2 (0.5)	5.55	3.78

Table 1: Overview of the light quark bare mass, $a\mu_\ell = a\mu_u = a\mu_d$, of the pion mass M_π , of the lattice size L and of the product $M_\pi L$ for the various ETMC gauge ensembles used in this work. The values of the lattice spacing a and the values of M_π and L correspond to the absolute scale $w_0 = 0.17383(63)$ fm.

1. Introduction

Precise and accurate scale setting is of central importance as lattice QCD calculations target high precision determinations of the hadron spectrum, the nucleon axial radius, precision inputs for electroweak tests of the Standard Model or the hadronic contribution to the muon $g - 2$. The lattice scale may enter either relatively to compare calculations at different values of the inverse bare coupling $\beta = 6/g_0^2$, indirectly when used to fix other bare parameters of the theory such as the quark masses or as an absolute scale in the conversion of dimensionful observables to physical units. Depending on the case, its uncertainty either indirectly or directly also propagates to the error estimates of the final results of a given calculation.

The gluonic scales t_0 [1] and w_0 [2] have been employed widely as intermediate scales [3–12] and have also previously been studied specifically in the context of the ETMC [13–15]. They are attractive because they are comparatively easy to calculate with high statistical precision, do not involve complicated fitting procedures and can easily be integrated into the ensemble production workflow. In this contribution we give some details on our current determinations of these scales and also present our recent calculation of f_K/f_π [16]. We also make use of the scales in the calculation of quark masses from mesonic inputs [17, 18] as well as leptonic meson decay constants [19].

2. Lattice Setup and Statistical Properties

We make use of $N_f = 2 + 1 + 1$ flavours of Wilson-clover twisted-mass fermions tuned to maximal twist, ensuring automatic $\mathcal{O}(a)$ -improvement of all physical observables [20, 21]. We employ the tmLQCD software suite [22–24] linked against an extended version of the QPhiX [25–30] library as well as DD α AMG [31–34]. Details of our ensembles are given in Table 1 and we refer to Refs.[15, 16, 35] for details on their generation and the corresponding algorithmic setup.

We employ the gradient flow using the Wilson gauge action and use a third-order Runge-Kutta algorithm as proposed in Ref. [1] to evolve the gauge field along the flow time t/a^2 . For the definition of the energy density $\langle E(t) \rangle$ in our observables, we make use of the clover discretisation of the field tensor, using the notation $\langle E_{\text{sym}}(t) \rangle$ in what follows. In Figure 1, we show the evolution of $t^2 \langle E_{\text{sym}}(t) \rangle$ and the corresponding MD history of the observable at the point $t = t_0^{\text{sym}}$ on ensemble *cC211.06.80* at the physical point as a representative example across our ensemble landscape.

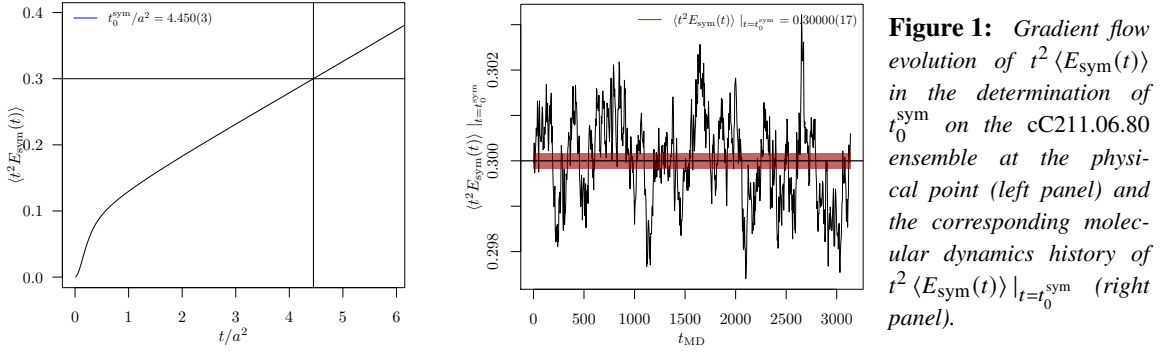


Figure 1: Gradient flow evolution of $t^2 \langle E_{\text{sym}}(t) \rangle$ in the determination of t_0^{sym} on the cC211.06.80 ensemble at the physical point (left panel) and the corresponding molecular dynamics history of $t^2 \langle E_{\text{sym}}(t) \rangle|_{t=t_0^{\text{sym}}}$ (right panel).

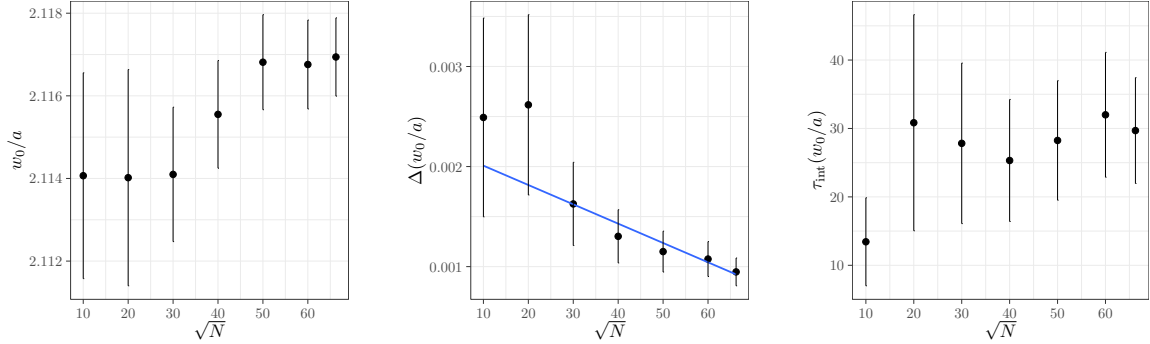


Figure 2: Scaling with the number of trajectories N (of length $\tau = 1.5$) of w_0/a (left), its statistical error (middle) and the estimate of the integrated autocorrelation time (right, in units of $\tau = 1.0$ trajectories) in an analysis on ensemble cB211.14.64. The blue line in the middle panel is a linear fit in the range $30 \leq \sqrt{N} \leq 60$.

We use the Gamma method [36] to estimate our statistical errors. While we do not estimate the exponential tails [37] of the autocorrelation function of our gradient flow observables, we see good error scaling and stable estimates of the integrated autocorrelation time. This is shown exemplarily in Figure 2 for the cB211.14.64 ensemble at a pion mass of around 190 MeV, where we give the evolution as a function of the number of trajectories N (of length $\tau = 1.5$) of the observable w_0/a , its statistical error and the corresponding estimate of the integrated autocorrelation time. These appear to be reliable from around $\sqrt{N} \sim 30$ onwards.

The results for all observables using the clover discretisation are given in Table 2, where we make use of the shorthand notation $s_0 = \sqrt{t_0}$.

3. Extrapolation to the Physical Point

Before we use the relative scales for further analysis, we follow Ref. [38] and extrapolate to the physical light quark mass at each lattice spacing. Since we have fixed the sea strange and charm quark masses to their physical values to within a few percent, we only parameterise the light quark mass dependence via

$$w_0/w_0^{\text{phys}}(\beta) = 1 + c_\beta \cdot \left[(M_{\text{PS}}/f_{\text{PS}})^2 - (M_\pi^{\text{iso}}/f_\pi^{\text{iso}})^2 \right], \quad (1)$$

where w_0^{phys}/a and c_β are fit parameters and where the pion mass M_{PS} and pion decay constant f_{PS} have been corrected for finite size effects as detailed in Ref. [16]. The quantities M_π^{iso} and f_π^{iso}

ensemble	N_{traj}	N_{meas}	s_0^{sym}/a	w_0^{sym}/a	$(t_0^{\text{sym}}/w_0^{\text{sym}})/a$	$s_0^{\text{sym}}/w_0^{\text{sym}}$	$\tau_{\text{int}}^{s_0}$	$\tau_{\text{int}}^{w_0}$	$\tau_{\text{int}}^{t_0/w_0}$	$\tau_{\text{int}}^{s_0/w_0}$
cA211.53.24	4488	1122	1.5306(21)	1.7597(43)	1.33139(89)	0.86982(100)	23(6)	25(7)	7(1)	18(4)
cA211.40.24	4876	1219	1.5384(18)	1.7766(33)	1.33213(96)	0.86592(64)	20(5)	18(4)	7(1)	9(2)
cA211.30.32	10236	2559	1.5460(9)	1.7928(17)	1.33314(47)	0.86233(32)	22(5)	21(4)	9(1)	10(2)
cA211.12.48	2608	326	1.5614(22)	1.8249(33)	1.33590(155)	0.85559(29)	69(30)	63(27)	59(25)	16(5)
cB211.25.24	4580	1145	1.7937(22)	2.0992(46)	1.53260(108)	0.85445(77)	21(5)	25(6)	5(1)	12(2)
cB211.25.32	3960	990	1.7922(19)	2.0991(47)	1.53018(72)	0.85380(91)	35(10)	45(14)	6(1)	28(7)
cB211.25.48	4700	1175	1.7915(8)	2.0982(19)	1.52966(41)	0.85384(38)	28(8)	31(9)	9(2)	20(5)
cB211.14.64	4952	619	1.7992(5)	2.1175(11)	1.52875(23)	0.84968(23)	30(8)	32(9)	8(1)	23(6)
cB211.072.64	3065	191	1.8028(8)	2.1272(19)	1.52784(42)	0.84750(41)	45(18)	52(22)	16(5)	41(16)
cC211.06.80	3140	785	2.1094(8)	2.5045(17)	1.77670(37)	0.84226(27)	46(17)	42(16)	14(3)	26(8)

Table 2: GF scales from the symmetrized action density and corresponding integrated autocorrelation times in units of trajectories of length $\tau = 1.0$. The N_{meas} measurements on each ensemble were performed using different separations in terms of trajectories and the τ_{int} were scaled appropriately. Similarly, for the cB211.25.24, cB211.25.32 and cB211.14.64 ensembles, the τ_{int} were scaled to take into account the $\tau = 1.5$ trajectory lengths used there.

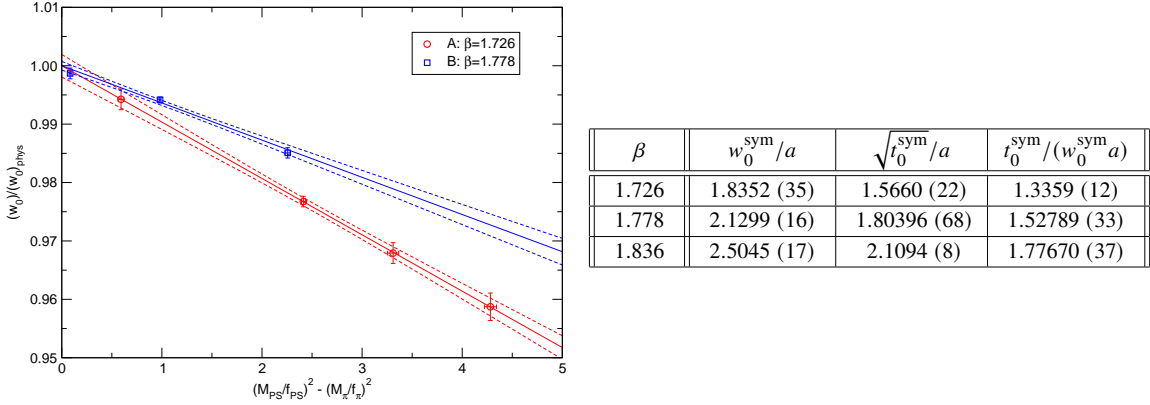


Figure 3: Extrapolation to the physical sea light quark mass of w_0/a at each lattice spacing using Equation (1) (left) and resulting values of all the relative scales at the physical point (right).

correspond to these quantities in the isosymmetric limit of QCD. The quality of the fit is shown for w_0^{sym}/a in the left panel of Figure 3 and the resulting values of all the relative scales at the physical point are given in the right panel. While we cannot perform this fit for our finest lattice spacing, the single ensemble there is very close to the physical point and we simply use the relative scales as they are.

4. Setting the Scale

We first attempt to set the scale via the pion decay constant directly, fitting the data for $w_0 f_\pi(L \rightarrow \infty)$ (which has been corrected for finite size effects) using the following functional form

$$w_0 f_\pi(L \rightarrow \infty) = w_0 f \left[1 - 2\xi \log(\xi) + 2A_1 \xi + A_2 \xi^2 + \frac{a^2}{w_0^2} (D_0 + D_1 \xi) \right], \quad (2)$$

where ξ is defined as

$$\xi \equiv \frac{M_\pi^2(L \rightarrow \infty)}{(4\pi f)^2} = \frac{(w_0 M_\pi)^2}{(4\pi w_0 f)^2} \frac{1}{\left[1 - \frac{1}{4} \Delta_\pi^{\text{FVE}}(L)\right]^2}, \quad (3)$$

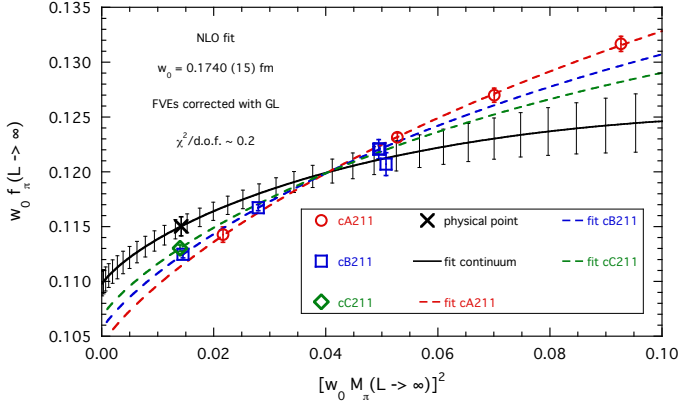


Figure 4: Fit of Equation (2) with $A_2 = 0$ to the data for $w_0 f_\pi$.

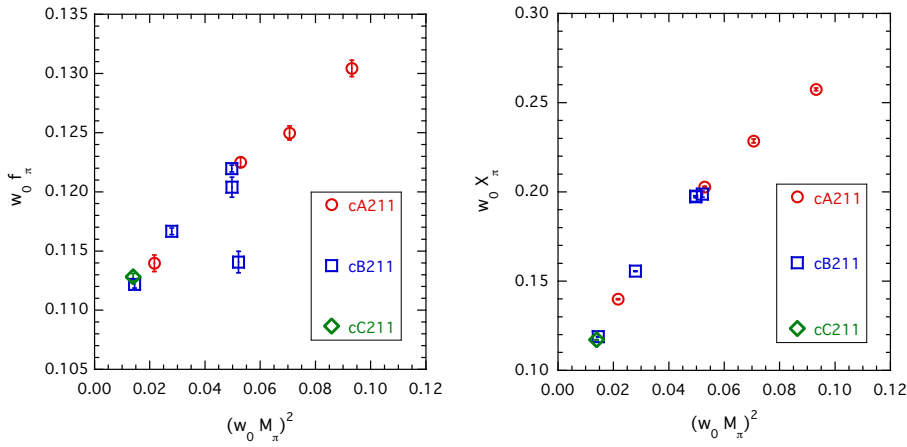


Figure 5: Raw data for the quantities $w_0 f_\pi$ (left) and $w_0 X_\pi$ (right, defined in Equation (4)).

and where, with respect to a pure NLO ansatz, we have added a possible higher-order term quadratic in ξ as well as discretization effects proportional to a^2 and $a^2 M_\pi^2$. For details we refer to Ref. [16] and show the fit with $A_2 = 0$ in Figure 4 with the result $w_0 = 0.1740(15)$ fm, corresponding to an 0.8% error.

In order to better exploit statistical correlations in the data for f_{PS} and M_{PS} as well as cancellations of discretisation and finite size effects, we consider the quantity

$$X_\pi = \left(f_\pi M_\pi^4 \right)^{1/5}, \quad (4)$$

for which we compare the raw data for $w_0 f_{PS}$ in the left panel of Figure 5 to the raw data for $w_0 X_{PS}$ in the right panel. It is clear that especially the finite size effects are greatly reduced in this combination. We proceed to fit

$$w_0 X_\pi = (w_0 f) \left\{ (4\pi)^4 \xi^2 \left[1 - 2\xi \log(\xi) + 2A_1 \xi + A_2' \xi^2 + a^2 (D_0' + D_1' \xi) \right] \right\}^{1/5} \cdot \left(1 + F_{\text{FVE}} \xi^2 e^{-M_\pi L} / (M_\pi L)^{3/2} \right), \quad (5)$$

the result of which is shown in the left panel of Figure 6. In the right panel, instead, we have subtracted the resulting continuum curve to better visualise the residual lattice artefacts which are very small and yet very well captured by the fit.

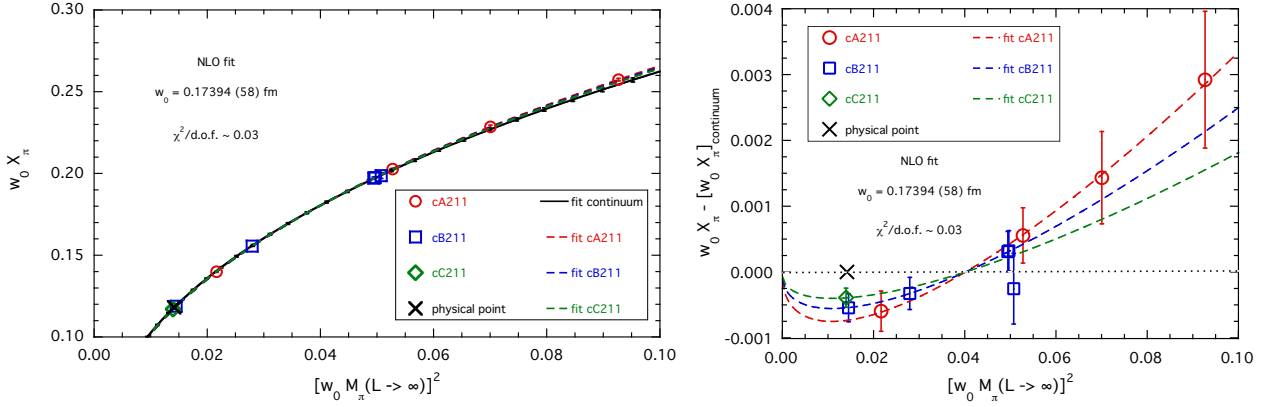


Figure 6: Fit of Equation (5) to the data for $w_0 X_\pi = w_0 (f_\pi M_\pi^4)^{(1/5)}$ (left) and detail with the resulting continuum curve subtracted to better visualise the very small residual lattice artefacts (right).

scale	$a_A(\beta = 1.726)$	$a_B(\beta = 1.778)$	$a_C(\beta = 1.836)$
w_0	0.09471(39)	0.08161(30)	0.06941(26)
$\sqrt{t_0}$	0.09217(41)	0.08002(34)	0.06844(29)
t_0/w_0	0.08960(47)	0.07834(41)	0.06737(35)

Table 3: Values of the lattice spacing a (in fm) corresponding to the three GF scales w_0 , $\sqrt{t_0}$, t_0/w_0 and to the corresponding relative scales given in the right panel of Figure 3.

For details we again refer to Ref. [16], where different cuts in the data and variations of the higher order terms are used to obtain estimates of systematic errors. Repeating the fits for the scales w_0 , t_0 and t_0/w_0 , we obtain

$$w_0 = 0.17383 (57)_{\text{stat+fit}} (26)_{\text{syst}} [63] \text{ fm}, \quad (6)$$

$$\sqrt{t_0} = 0.14436 (54)_{\text{stat+fit}} (30)_{\text{syst}} [61] \text{ fm}, \quad (7)$$

$$t_0/w_0 = 0.11969 (52)_{\text{stat+fit}} (33)_{\text{syst}} [62] \text{ fm}, \quad (8)$$

with errors added in quadrature and given in square brackets, resulting in an improvement in precision by a factor of about 2.5 compared to the determination from f_π .

The values of the lattice spacing a corresponding to Equations (6) to (8) are given in Table 3. These three determinations of a differ by $\mathcal{O}(a^2)$ effects, which can be parameterised in their ratios by a function linear in a^2 , as shown in Fig. 7. In particular, we get: $a(\sqrt{t_0})/a(w_0) \simeq 1 - 0.09 (2) a^2(w_0)/w_0^2$ and $a(t_0/w_0)/a(w_0) \simeq 1 - 0.18 (2) a^2(w_0)/w_0^2$, consistent with a^2 -scaling.

5. The ratio f_K/f_π

Finally, we employ the lattice spacing determined via w_0/a and fixed by X_π to interpolate our data for f_K/f_π to a reference kaon mass $(M_K^{\text{ref}})^2 = (M_K^{\text{iso}})^2 + (M_\pi^2 - M_\pi^{\text{iso}2})/2$. This interpolated data for f_K/f_π is shown in Figure 8. We further apply finite size corrections as detailed in Ref. [16] and the data using the Ansatz

$$\frac{f_K}{f_\pi}(L \rightarrow \infty) = R_0 \left[1 + \frac{5}{4} \xi \log(\xi) + R_1 \xi + R_2 \xi^2 + \frac{a^2}{w_0^2} (\tilde{D}_0 + \tilde{D}_1 \xi) \right]. \quad (9)$$

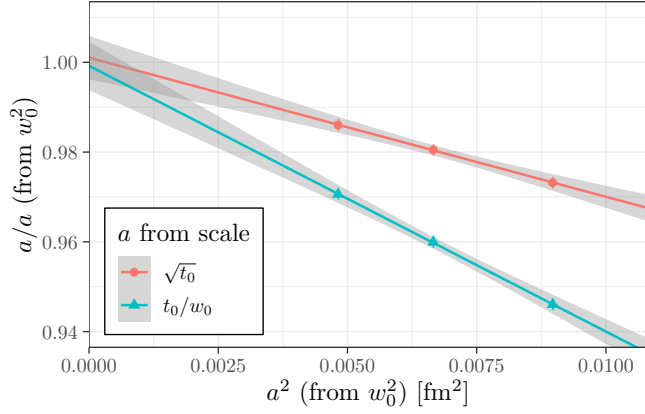


Figure 7: Ratios of lattice spacings determined via $\sqrt{t_0}$ and t_0/w_0 with the lattice spacing determined via w_0 with linear fits superimposed.

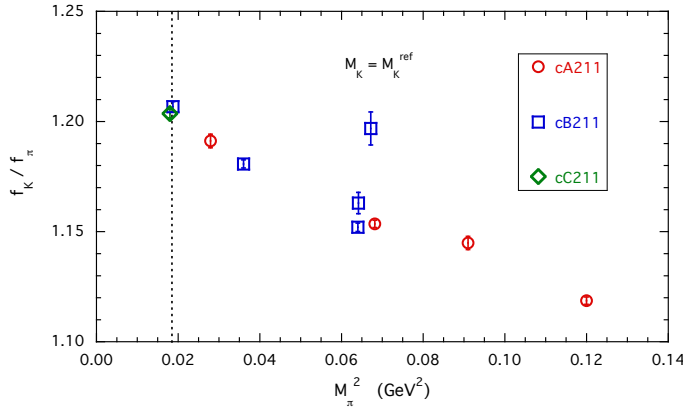


Figure 8: Data for f_K/f_π on all ensembles used in this work interpolated to the reference kaon mass $(M_K^{\text{ref}})^2 = (M_K^{\text{iso}})^2 + (M_\pi^2 - M_\pi^{\text{iso}})^2/2$.

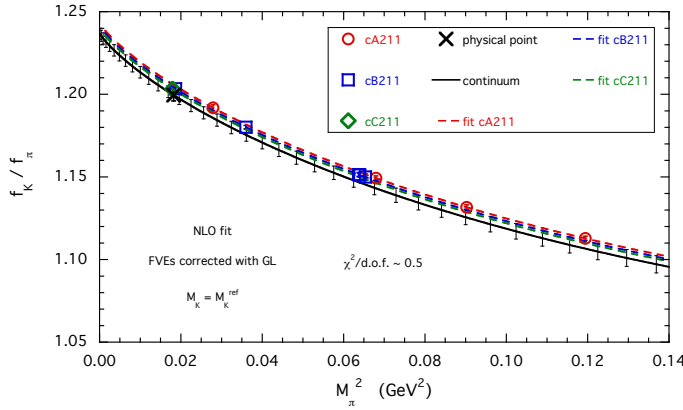


Figure 9: Fit of Equation (9) to the f_K/f_π data shown in Figure 8 corrected for finite size effects.

As shown in Figure 9, this results in an excellent fit and we obtain

$$\left(\frac{f_K}{f_\pi}\right)^{\text{iso}} = 1.1995 (44)_{\text{stat+fit}} (7)_{\text{syst}} [44], \quad (10)$$

at the physical point in the isosymmetric limit of QCD, where again, estimates of the systematic errors are obtained by performing different types of fits and data cuts.

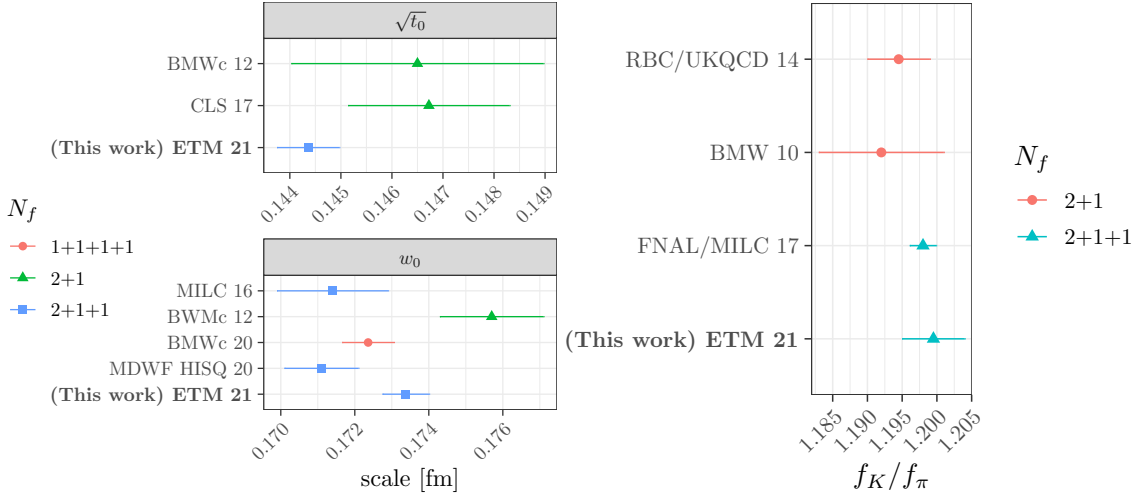


Figure 10: Comparison of the results of this work for the scales w_0 and $\sqrt{t_0}$ from Refs. [2, 8–10, 12] (left panel) and for f_K/f_π to those from Refs. [39–41] (right panel).

6. Conclusions and Outlook

We conclude by comparing our results for the scales w_0 and $\sqrt{t_0}$ to an incomplete selection from Refs. [2, 8–10, 12] in the left panel of Figure 10 and our result for f_K/f_π to a selection from Refs. [39–41] in the right panel. For more complete comparisons we refer to the FLAG review [42]. In future publications we plan to extend the set of ensembles by simulations at a fourth lattice spacing, several more volumes and further values of the light sea quark mass at $\beta = 1.836$. An alternative scale setting employing the mass of the omega baryon is currently being studied with the aim of also including QED effects.

Acknowledgments

We thank all the ETMC members for a very productive collaboration.

We acknowledge PRACE for access to Marconi and Marconi100 at CINECA under the grants Pra17-4394, Pra20-5171 and Pra22-5171, and CINECA for providing us CPU time under the specific initiative INFN-LQCD123. We also acknowledge PRACE for awarding us access to HAWK, hosted by HLRS, Germany, under the grant with id 33037. The authors gratefully acknowledge the Gauss Centre for Supercomputing e.V. (www.gauss-centre.eu) for funding the project pr74yo by providing computing time on the GCS Supercomputer SuperMUC at Leibniz Supercomputing Centre (www.lrz.de). Some of the ensembles for this study were generated on Jureca Booster [43] and Juwels [44] at the Jülich Supercomputing Centre (JSC) and we gratefully acknowledge the computing time granted there by the John von Neumann Institute for Computing (NIC). We also acknowledge access to the Bonna HPC Cluster at the University of Bonn.

The project has received funding from the Horizon 2020 research and innovation program of the European Commission under the Marie Skłodowska-Curie grant agreement No 642069 (HPC-LEAP) and under grant agreement No 765048 (STIMULATE). The project was funded in part by the NSFC (National Natural Science Foundation of China) and the DFG (Deutsche Forschungsgemeinschaft, German Research Foundation) through the Sino-German Collaborative Research Center grant TRR110 ‘‘Symmetries and the Emergence of Structure in QCD’’ (NSFC Grant No. 12070131001, DFG Project-ID 196253076 - TRR 110).

R.F. acknowledges support from the University of Tor Vergata through the Grant ‘‘Strong Interactions: from Lattice QCD to Strings, Branes and Holography’’ within the Excellence Scheme ‘‘Beyond the Borders’’ F.S. and S.S. are supported by the Italian Ministry of Research (MIUR) under grant PRIN 20172LNEEZ. F.S. is supported by INFN

under GRANT73/CALAT. P.D. acknowledges support from the European Unions Horizon 2020 research and innovation programme under the Marie Skłodowska-Curie grant agreement No. 813942 (EuroPLEx) and from INFN. under the research project INFN-QCDLAT. S.B. and J.F. are supported by the H2020 project PRACE6-IP (grant agreement No 82376) and the COMPLEMENTARY/0916/0015 project funded by the Cyprus Research Promotion Foundation. The authors acknowledge support from project NextQCD, co-funded by the European Regional Development Fund and the Republic of Cyprus through the Research and Innovation Foundation (EXCELLENCE/0918/0129).

References

- [1] M. Lüscher, *Properties and uses of the Wilson flow in lattice QCD*, *JHEP* **08** (2010) 071 [1006.4518].
- [2] S. Borsanyi et al., *High-precision scale setting in lattice QCD*, *JHEP* **09** (2012) 010 [1203.4469].
- [3] ALPHA collaboration, *On the N_f -dependence of gluonic observables*, *PoS LATTICE2013* (2014) 321 [1311.5585].
- [4] R.J. Dowdall, C.T.H. Davies, G.P. Lepage and C. McNeile, *Vus from pi and K decay constants in full lattice QCD with physical u, d, s and c quarks*, *Phys. Rev. D* **88** (2013) 074504 [1303.1670].
- [5] V.G. Bornyakov et al., *Wilson flow and scale setting from lattice QCD*, 1508.05916.
- [6] HorQCD collaboration, *Equation of state in $(2+1)$ -flavor QCD*, *Phys. Rev. D* **90** (2014) 094503 [1407.6387].
- [7] RBC, UKQCD collaboration, *Domain wall QCD with physical quark masses*, *Phys. Rev. D* **93** (2016) 074505 [1411.7017].
- [8] MILC collaboration, *Gradient flow and scale setting on MILC HISQ ensembles*, *Phys. Rev. D* **93** (2016) 094510 [1503.02769].
- [9] M. Bruno, T. Korzec and S. Schaefer, *Setting the scale for the CLS $2 + 1$ flavor ensembles*, *Phys. Rev. D* **95** (2017) 074504 [1608.08900].
- [10] N. Miller et al., *Scale setting the Möbius domain wall fermion on gradient-flowed HISQ action using the omega baryon mass and the gradient-flow scales t_0 and w_0* , *Phys. Rev. D* **103** (2021) 054511 [2011.12166].
- [11] ALPHA collaboration, *Scale setting for $N_f = 3 + 1$ QCD*, *Eur. Phys. J. C* **80** (2020) 349 [2002.02866].
- [12] S. Borsanyi et al., *Leading hadronic contribution to the muon magnetic moment from lattice QCD*, *Nature* **593** (2021) 51 [2002.12347].
- [13] A. Deuzeman and U. Wenger, *Gradient flow and scale setting for twisted mass fermions*, *PoS LATTICE2012* (2012) 162.
- [14] ETM collaboration, *First physics results at the physical pion mass from $N_f = 2$ Wilson twisted mass fermions at maximal twist*, *Phys. Rev. D* **95** (2017) 094515 [1507.05068].
- [15] C. Alexandrou et al., *Simulating twisted mass fermions at physical light, strange and charm quark masses*, *Phys. Rev. D* **98** (2018) 054518 [1807.00495].
- [16] EXTENDED TWISTED MASS collaboration, *Ratio of kaon and pion leptonic decay constants with $N_f=2+1+1$ Wilson-clover twisted-mass fermions*, *Phys. Rev. D* **104** (2021) 074520 [2104.06747].
- [17] EXTENDED TWISTED MASS collaboration, *Quark masses using twisted-mass fermion gauge ensembles*, *Phys. Rev. D* **104** (2021) 074515 [2104.13408].
- [18] C. Alexandrou et al., *Determination of the light, strange and charm quark masses using twisted mass fermions*, *PoS LATTICE2021* (2021) 171 [2110.04588].
- [19] P. Dimopoulos, R. Frezzotti, M. Garofalo and S. Simula, *K - and $D_{(s)}$ -meson leptonic decay constants with physical light, strange and charm quarks by ETMC*, *PoS LATTICE2021* (2021) 472 [2110.01294].
- [20] ALPHA collaboration, *$O(a)$ improved twisted mass lattice QCD*, *JHEP* **07** (2001) 048 [hep-lat/0104014].
- [21] R. Frezzotti and G.C. Rossi, *Chirally improving Wilson fermions. I. $O(a)$ improvement*, *JHEP* **08** (2004) 007 [hep-lat/0306014].
- [22] K. Jansen and C. Urbach, *tmLQCD: A Program suite to simulate Wilson Twisted mass Lattice QCD*, *Comput. Phys. Commun.* **180** (2009) 2717 [0905.3331].

- [23] A. Abdel-Rehim, F. Burger, A. Deuzeman, K. Jansen, B. Kostrzewa, L. Scorzato et al., *Recent developments in the tmLQCD software suite*, *PoS LATTICE2013* (2014) 414 [1311.5495].
- [24] A. Deuzeman, K. Jansen, B. Kostrzewa and C. Urbach, *Experiences with OpenMP in tmLQCD*, *PoS LATTICE2013* (2014) 416 [1311.4521].
- [25] B. Joó, D. Kalamakar, K. Vaidyanathan, M. Smelyanskiy, T. Kurth, A. Walden et al. <https://github.com/JeffersonLab/qphix>.
- [26] B. Joó, D.D. Kalamkar, K. Vaidyanathan, M. Smelyanskiy, K. Pamnany, V.W. Lee et al., *Lattice qcd on intel® xeon phi™ coprocessors*, in *Supercomputing*, J.M. Kunkel, T. Ludwig and H.W. Meuer, eds., (Berlin, Heidelberg), pp. 40–54, Springer Berlin Heidelberg, 2013.
- [27] M. Schröck, S. Simula and A. Strelchenko, *Accelerating Twisted Mass LQCD with QPhiX*, *PoS LATTICE2015* (2016) 030 [1510.08879].
- [28] B. Joó, D.D. Kalamkar, T. Kurth, K. Vaidyanathan and A. Walden, *Optimizing wilson-dirac operator and linear solvers for intel® knl*, in *International Conference on High Performance Computing*, pp. 415–427, Springer, 2016.
- [29] B. Joo, M. Smelyanskiy, D.D. Kalamkar and K. Vaidyanathan, *Wilson dslash kernel from lattice qcd optimization*, Tech. Rep. Thomas Jefferson National Accelerator Facility (TJNAF), Newport News, VA . . . (2015).
- [30] S. Heybrock, B. Joó, D.D. Kalamkar, M. Smelyanskiy, K. Vaidyanathan, T. Wettig et al., *Lattice qcd with domain decomposition on intel® xeon phi co-processors*, in *SC '14: Proceedings of the International Conference for High Performance Computing, Networking, Storage and Analysis*, pp. 69–80, 2014, DOI.
- [31] A. Frommer, K. Kahl, S. Krieg, B. Leder and M. Rottmann, *Adaptive Aggregation Based Domain Decomposition Multigrid for the Lattice Wilson Dirac Operator*, *SIAM J. Sci. Comput.* **36** (2014) A1581 [1303.1377].
- [32] A. Frommer, K. Kahl, S. Krieg, B. Leder and M. Rottmann, *An adaptive aggregation based domain decomposition multilevel method for the lattice wilson dirac operator: multilevel results*, 1307.6101.
- [33] C. Alexandrou, S. Bacchio, J. Finkenrath, A. Frommer, K. Kahl and M. Rottmann, *Adaptive Aggregation-based Domain Decomposition Multigrid for Twisted Mass Fermions*, *Phys. Rev. D* **94** (2016) 114509 [1610.02370].
- [34] C. Alexandrou, S. Bacchio and J. Finkenrath, *Multigrid approach in shifted linear systems for the non-degenerated twisted mass operator*, *Comput. Phys. Commun.* **236** (2019) 51 [1805.09584].
- [35] J. Finkenrath, C. Alexandrou, S. Bacchio, P. Dimopoulos, R. Frezzotti, K. Jansen et al., *Twisted mass gauge ensembles at physical values of the light, strange and charm quark masses*, *PoS LATTICE2021* (2021) 284.
- [36] ALPHA collaboration, *Monte Carlo errors with less errors*, *Comput. Phys. Commun.* **156** (2004) 143 [hep-lat/0306017].
- [37] ALPHA collaboration, *Critical slowing down and error analysis in lattice QCD simulations*, *Nucl. Phys. B* **845** (2011) 93 [1009.5228].
- [38] O. Bar and M. Golterman, *Chiral perturbation theory for gradient flow observables*, *Phys. Rev. D* **89** (2014) 034505 [1312.4999].
- [39] S. Dürr, Z. Fodor, C. Hoelbling, S.D. Katz, S. Krieg, T. Kurth et al., *Ratio F_K/F_π in qcd*, *Phys. Rev. D* **81** (2010) 054507.
- [40] RBC AND UKQCD COLLABORATIONS collaboration, *Domain wall qcd with physical quark masses*, *Phys. Rev. D* **93** (2016) 074505.
- [41] A. Bazavov et al., *B- and D-meson leptonic decay constants from four-flavor lattice QCD*, *Phys. Rev. D* **98** (2018) 074512 [1712.09262].
- [42] Y. Aoki et al., *FLAG Review 2021*, 2111.09849.
- [43] Jülich Supercomputing Centre *Journal of large-scale research facilities* **A132** (2018) .
- [44] Jülich Supercomputing Centre *Journal of large-scale research facilities* **A135** (2019) .